Kinetics of Reaction of *n*-Butanol and Triaminononane Trisisocyanate Measured via ^{13}C Solution NMR

M. R. KREJSA* and H. P. HIGGINBOTTOM

The Chemical Group of Monsanto, Indian Orchard Plant, 730 Worcester Street, Springfield, Massachusetts 01151

SYNOPSIS

The model reaction kinetics of a novel trifunctional isocyanate 4-aminomethyl-1,8-diaminooctane [informally referred to as triaminononane trisisocyanate (TTI)] with *n*-butanol is described. Butanol is used in place of the normal polyols used in actual coatings formulations in order to simplify the system for kinetic analysis. Using ^{13}C-NMR, the differences in reactivity of each isocyanate group was studied in real-time measurements. There is little difference in the second-order rate constants between the three TTI isocyanate groups in the uncatalyzed systems at 25, 35, or 45°C. The dibutyl tin dilaureate (DBTDL) catalyzed system exhibits similar second-order rate constants for the medium- and long-branch systems, and a smaller rate constant for the short-branch system. The activation energies increase with increasing chain length in the uncatalyzed system, while for the catalyzed system the long and medium branches have identical activation energies, and the short-branch system has the lowest activation energy. The addition of chloroform or increasing the butanol : TTI ratio results in an increase of the measured rate constant. © 1995 John Wiley & Sons, Inc.

INTRODUCTION

The use of aliphatic isocyanates in coating applications continues to grow because they offer excellent UV and weathering resistance along with other desirable coating properties. Coating applications now account for over 90% of the usage of aliphatic isocyanates. There is a strong impetus for the development of novel aliphatic isocyanates, particularly for use in low VOC coatings.[1] A trifunctional isocyanate, prepared by a patented nonphosgene process from 4-aminomethyl-1,8-diaminooctane has been recently described.[2,3] This triisocyanate is informally referred to as triaminononane trisisocyanate (TTI). TTI has extremely low viscosity (10 mPa s) and low equivalent weight (84 g/eq). Despite these characteristics, initial tests suggest that TTI is more similar to polyisocyanates than to hexamethylene diisocyanate in toxicological properties and performance in coating systems.[3] This similarity to polyisocyanates is especially emphasized by a very low vapor pressure of TTI (1.0×10^{-5} mm at 20°C). TTI offers the potential of very low or zero VOC when properly formulated into a coating system.

The focus of the research described in this article is to determine the reactivity of the isocyanate groups present in TTI. The potential exists in the case of TTI for different reactivity among three different length isocyanate-terminated aliphatic chains emanating from a center branch:

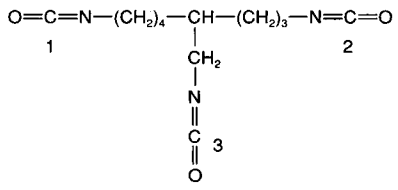

Triaminononane Trisisocyanate

These three branches will be referred to as the long (1), medium (2), and short (3) branches, respectively. This article will explore the reactivity differences, if any, of these three isocyanate groups. Our approach will be to use the model reaction of

* To whom correspondence should be addressed.

Journal of Applied Polymer Science, Vol. 58, 2141–2154 (1995)
 CCC 0021-8995/95/122141-14

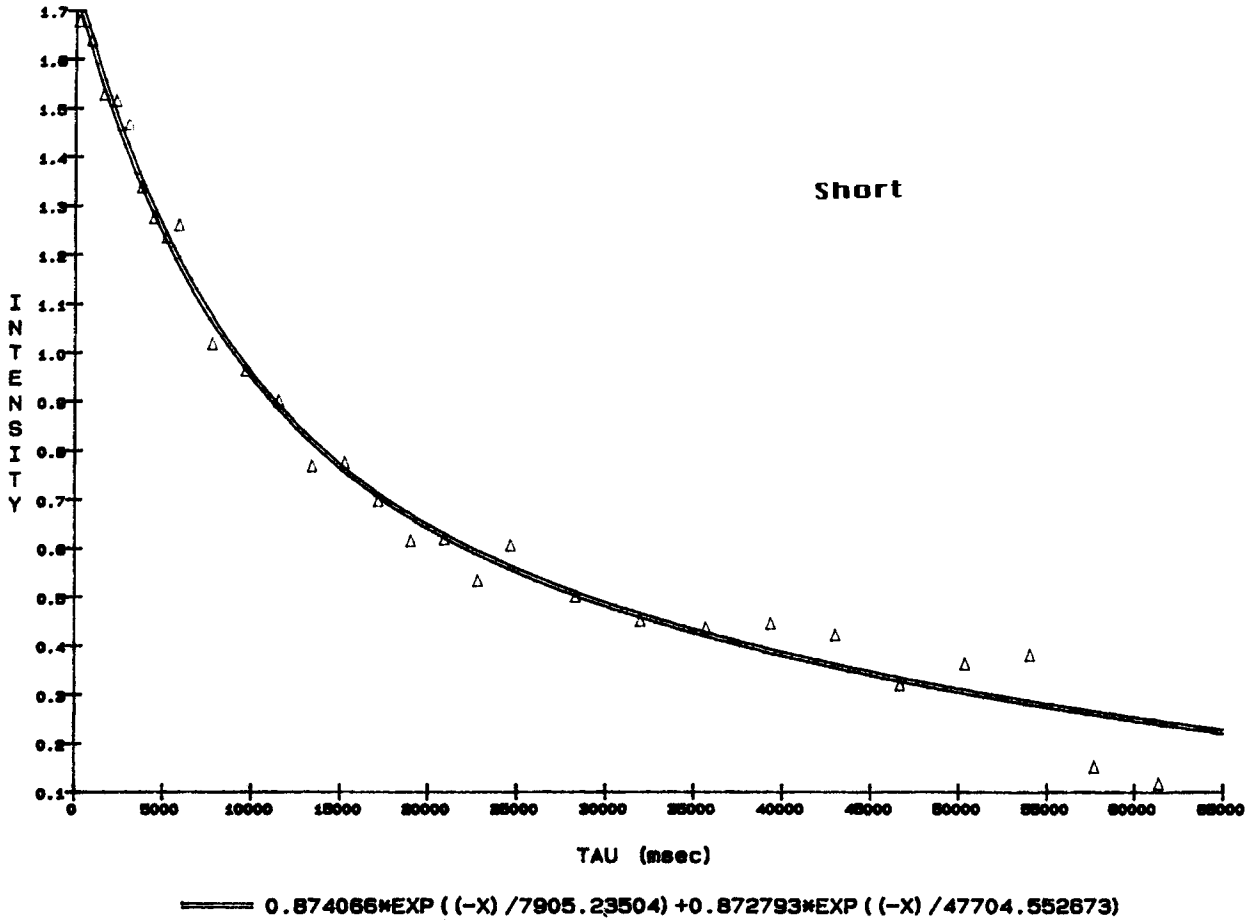

Figure 1 Plot of amount of each unreacted isocyanate group in TTI as a function of reaction time for the uncatalyzed system at 25°C. The empirical biexponential curve fits for each sample are shown.

n-butanol and TTI to avoid problems with gelation inherent in actual coating formulations. This reaction is shown below:

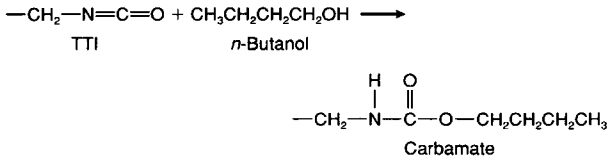

Additionally, the role of catalysis is of interest; our approach will be to study the system both catalyzed and uncatalyzed to determine how the reactivity is affected by catalysis. Additionally, we will briefly study the role of a solvent/compatibilizer (chloroform) and reactant ratio (*n*-butanol : TTI ratio) on the rate constants.

The usual approach to isocyanate kinetic studies is to work in dilute solutions and with an excess of one component (typically the alcohol). This approach has the advantage of removing any viscosity dependence from the measured rate constants, and also allows the reduction of the rate equations to first order. Additionally, many of the analytical techniques used are well suited to dilute solution conditions. Two of the most common techniques are infrared spectroscopy and titration. Infrared spectroscopy takes advantage of the strong extinction coefficient of the isocyanate functional group; however, IR is limited in the case of high concentrations, as the signal is no longer linearly related to concentration. The titration method involves quenching the reaction with di-*n*-butylamine, and then measuring the amount of consumed di-*n*-butylamine by titration. This is another technique well suited to dilute solutions. However, both techniques suffer from an inability to distinguish between chemically different isocyanate groups. Our approach to this problem was to use real-time ^{13}C solution NMR to measure the reaction kinetics of the TTI/*n*-butanol reaction. The ^{13}C-NMR spectrum of TTI has a unique peak for the methylene groups adjacent to

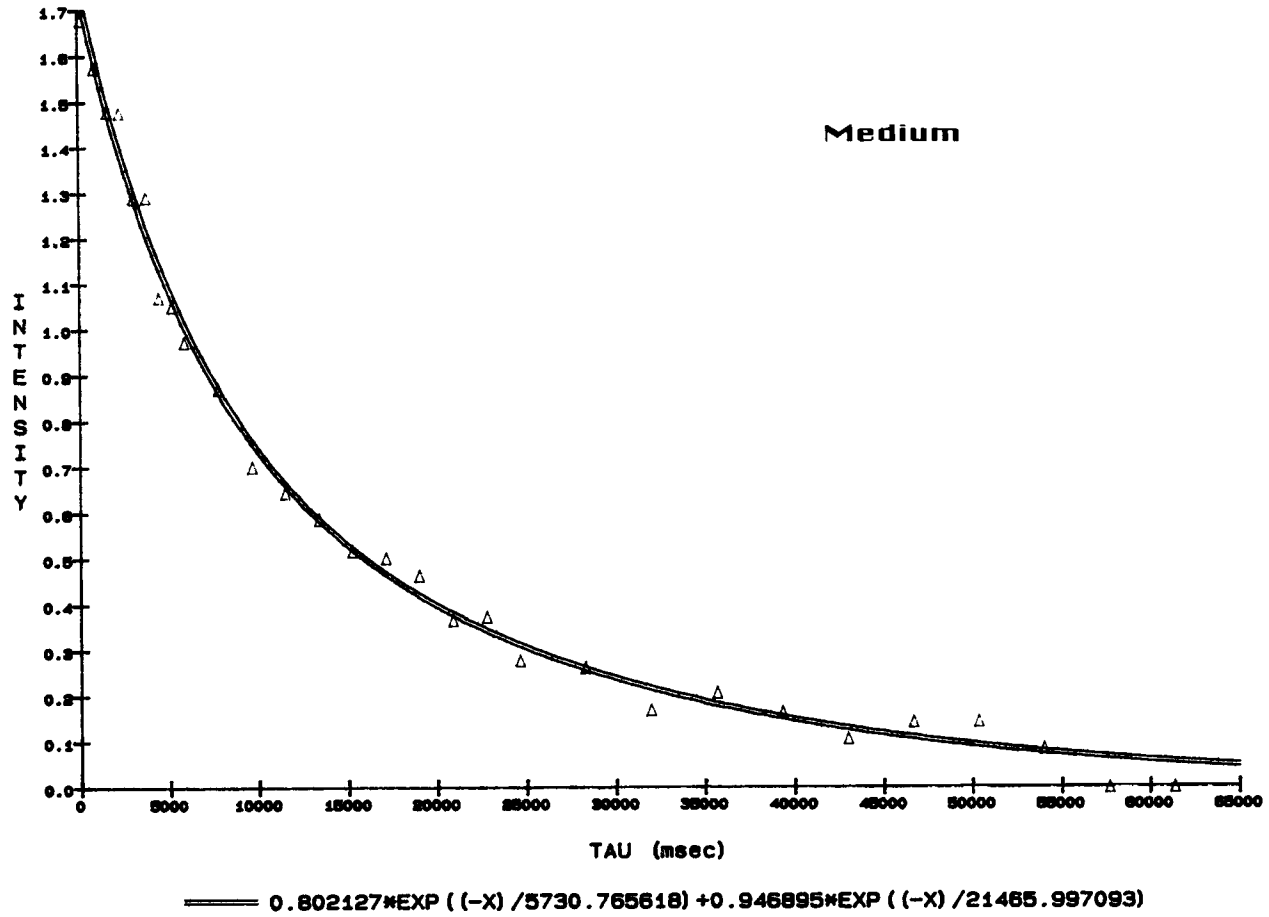

Figure 1 (*Continued from the previous page*)

the isocyanate functional moiety. This spectral separation allowed us to quantify the reaction kinetics for each isocyanate group in TTI, and further allowed the measurement of reaction rate under concentrations more representative of those found in actual coatings applications.

The use of ^{13}C solution NMR for measurement of kinetic constants of isocyanates is a methodology not readily found in the literature for isocyanate kinetic studies. The most common method of analysis of aliphatic isocyanate and aliphatic alcohol reactions is reacting the sample with di-*n*-butylamine.[4-9] The amount of unreacted di-*n*-butylamine is then titrated, and the difference between starting and final amount gives the amount of unreacted isocyanate. Seneker and Potter coupled the titration method with a refractive index method in which the refractive index is linearly related to unreacted isocyanate content; the calibration curve was constructed via titration data.[7] Another approach is the use of infrared spectroscopy to quantify the reduction in isocyanate content.[10-12] This method has the advantage of performing kinetics real time, but cannot distinguish between slightly different isocyanate groups. Surivet, Lam, and Pascault used Size Exclusion Chromatography to follow the reaction, and ^{13}C-NMR to quantify the final extent of reaction.[13] No direct references have been found of the use of ^{13}C-NMR to follow isocyanate kinetics real time.

EXPERIMENTAL

All samples for kinetic measurements were prepared in a 5 mm solution NMR tube for analysis on a Bruker AC-200 NMR spectrometer using a 5 mm solution probe. Samples for kinetic measurement were weighed directly in the NMR tube, and the tube inserted into the NMR magnet. The samples were run unlocked and spinning at 20 Hz using a standard ^{13}C Inverse Gated sequence (^{13}C 90° pulse with decoupling only during acquisition). The number of scans was either 16, 32, or 64, depending on the overall rate of reaction. The recycle delay was based on the measured ^{13}C T1 values to allow full relaxation of the carbons being quantified. ^{13}C T1

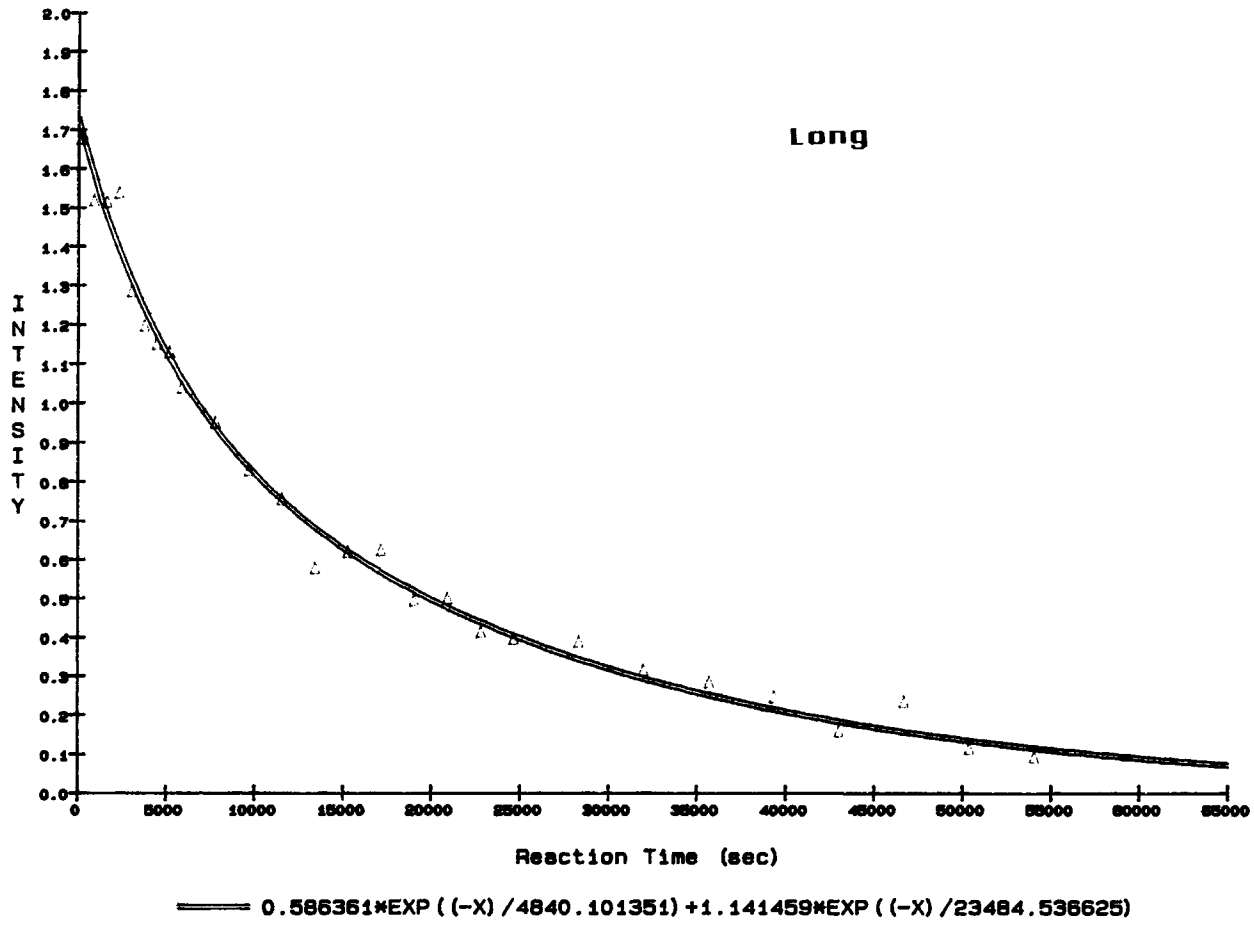

Figure 1 (*Continued from the previous page*)

measurements were performed on the same instrument using an inversion recovery pulse sequence (180-τ-90-AQ). The recycle delay was 15–20 s for the T1 measurements, the spectral width was 12500 Hz (248 ppm), and the spectral frequency was 50.323 MHz. The T1 data was fit using the equation

$$I(\tau) = A + B[1 - \exp(-\tau/T1)]$$

where A is the starting intensity, and the signal intensity varies from A to $A+B$. This form of the inversion recovery equation accounts for nonideal intensities. The ^{13}C and DEPT spectrum used for assignment of the TTI peaks was performed under similar conditions to the ^{13}C T1 measurements. The J(CH) used for the DEPT experiment was 140 Hz, and the recycle delay for this experiment was 5 s.

Kinetic measurements of the concentration of each unreacted isocyanate were taken using the methylene carbons adjacent to each isocyanate group. This will be discussed in detail in the Discussion section.

The kinetic calculations involving this system are complicated by the fact that the same alcohol can react with three different isocyanates at different rates, so a simple second-order equation cannot be used. Additionally, the system cannot be treated as a pseudofirst order, as the concentrations required to meet this condition would require too low a concentration for useful ^{13}C-NMR. These complications required each reaction to be plotted separately. The kinetic equations used were

$$[A_1] + [\text{BuOH}] \rightarrow [C_1] \quad (1)$$

$$[A_2] + [\text{BuOH}] \rightarrow [C_2] \quad (2)$$

$$[A_3] + [\text{BuOH}] \rightarrow [C_3] \quad (3)$$

where: A_i are the isocyanate groups, BuOH is the n-butanol, and C_i is the carbamate product.

From this, the basic kinetic equation is

$$\frac{-d[A_i]}{dt} = -k_i[A_i][\text{BuOH}] \quad (4)$$

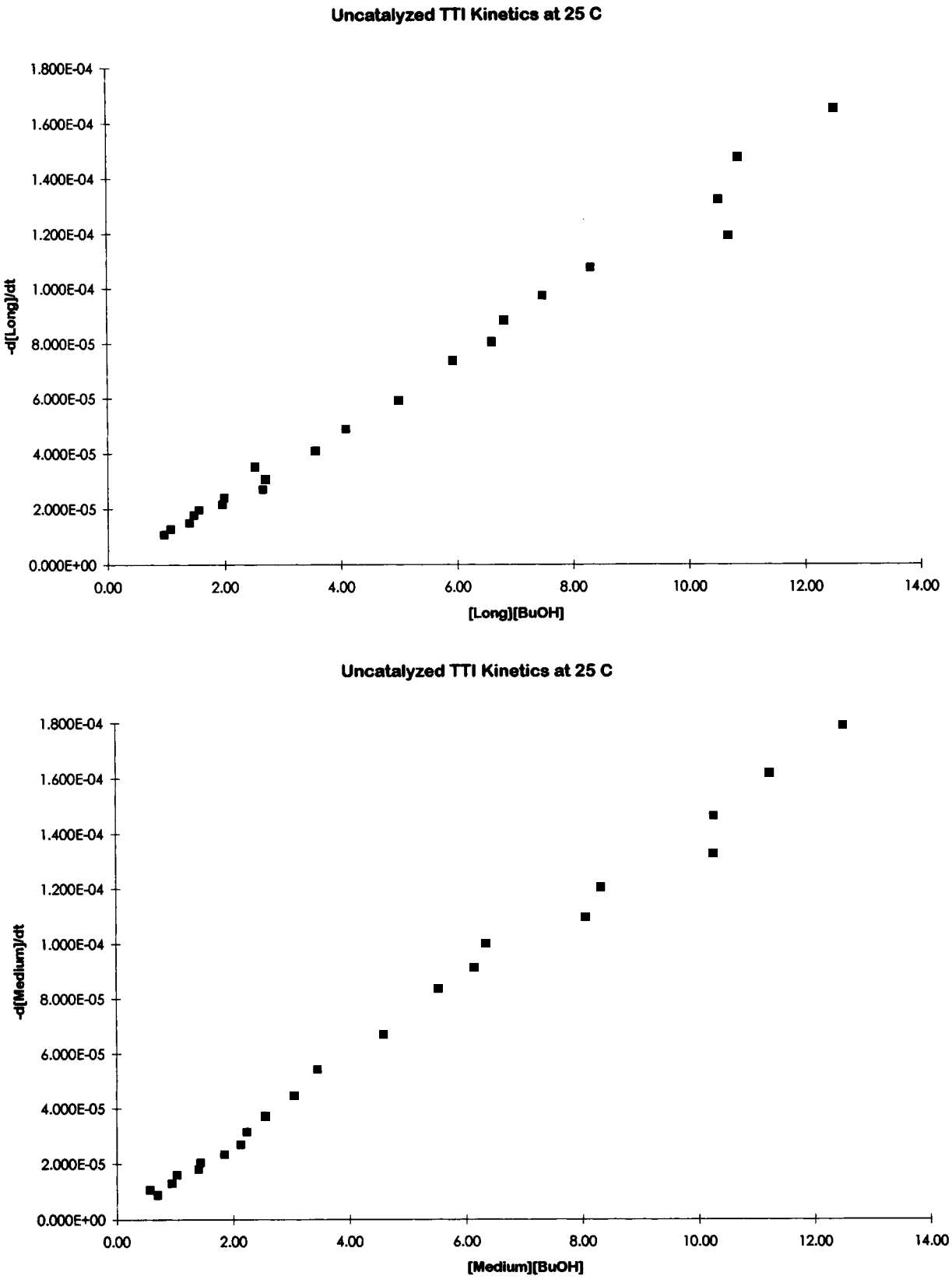

Figure 2 (a–c) Plots of $-d[A_i]/dt$ vs. k_i*[A_i]*[BuOH] for the uncatalyzed system at 25°C. Low conversion is at the right and high conversion at the left.

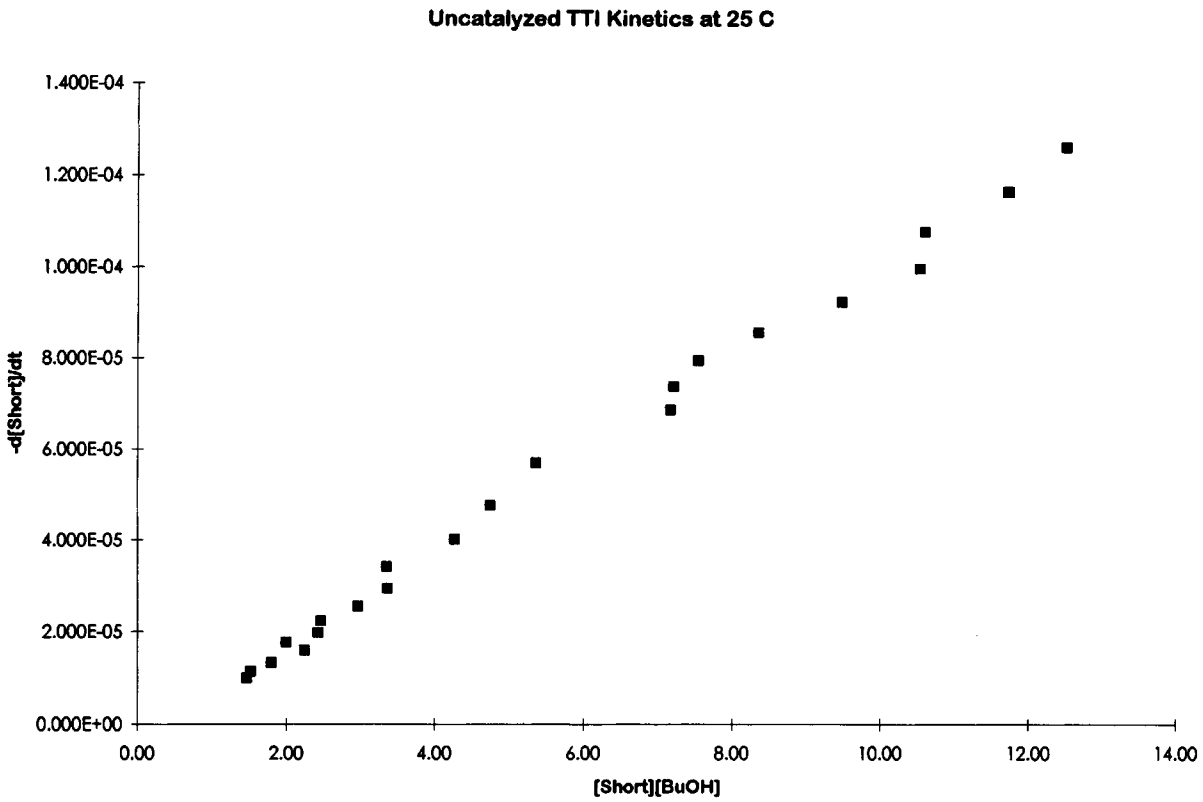

Figure 2 *(Continued from the previous page)*

Kinetic constants were calculated by plotting the intensity of each peak as a function of time, and then fitting the data as a biexponential curve for uncatalyzed systems, and a single exponential decay for catalyzed systems. This is shown in Figure 1(a–c) for the 25°C uncatalyzed system. These curves were then differentiated, and plotted vs. $[A_i]^*[B]$ giving a slope of k_i, as can be seen in Figure 2(a–c) for these same peaks. The second-order rate constants were calculated using the points down to a [NCO]*[BuOH] product of 3.5 or higher due to observed change in rate constant at higher conversions in many systems (conversion goes from high to low on this type of plot). The concentration of *n*-butanol was calculated by the initial concentration minus the decrease in each isocyanate functionality (via the adjacent methylene carbon). The *n*-butanol peaks were not quantified due to their very long ^{13}C T1 values.

Catalyzed kinetics were performed by adding the catalyst dibutyl tin dilaureate (DBTDL) to the chloroform solution in the proper concentration such that the catalyst concentration was 0.1 parts per 100 g of TTI. The chloroform was present as a 25% weight percent component in all systems as a compatibilizing agent, because the unreacted butanol–TTI system will segregate into separate components at low conversions.

The time value used for each individual NMR experiment was the starting point of that experiment. The starting time was taken as the moment at which the alcohol and isocyanate (and catalyst if applicable) were mixed; thus, each kinetic run has a 3–4 min lead time before the first measurement. The measurement temperature, which is crucial for kinetic experiments, reached equilibrium within 1–2 min after insertion of the tube into the NMR spectrometer. The measurement temperature was controlled to better than ± 0.1°C.

Chemical shift calculations were performed using Grant–Paul additivity rules. To calculate chemical shifts for isocyanates, additivity parameters for isocyanate groups were calculated from the literature ^{13}C-NMR spectra[13] of seven alkanes and their corresponding isocyanates. The calculated values are α(NCO) = +29.9, β(NCO) = +8.6, and δ(NCO) = −5.4 ppm.

RESULTS AND DISCUSSION

This research will be discussed in three sections. The first section is the NMR assignments of the ^{13}C

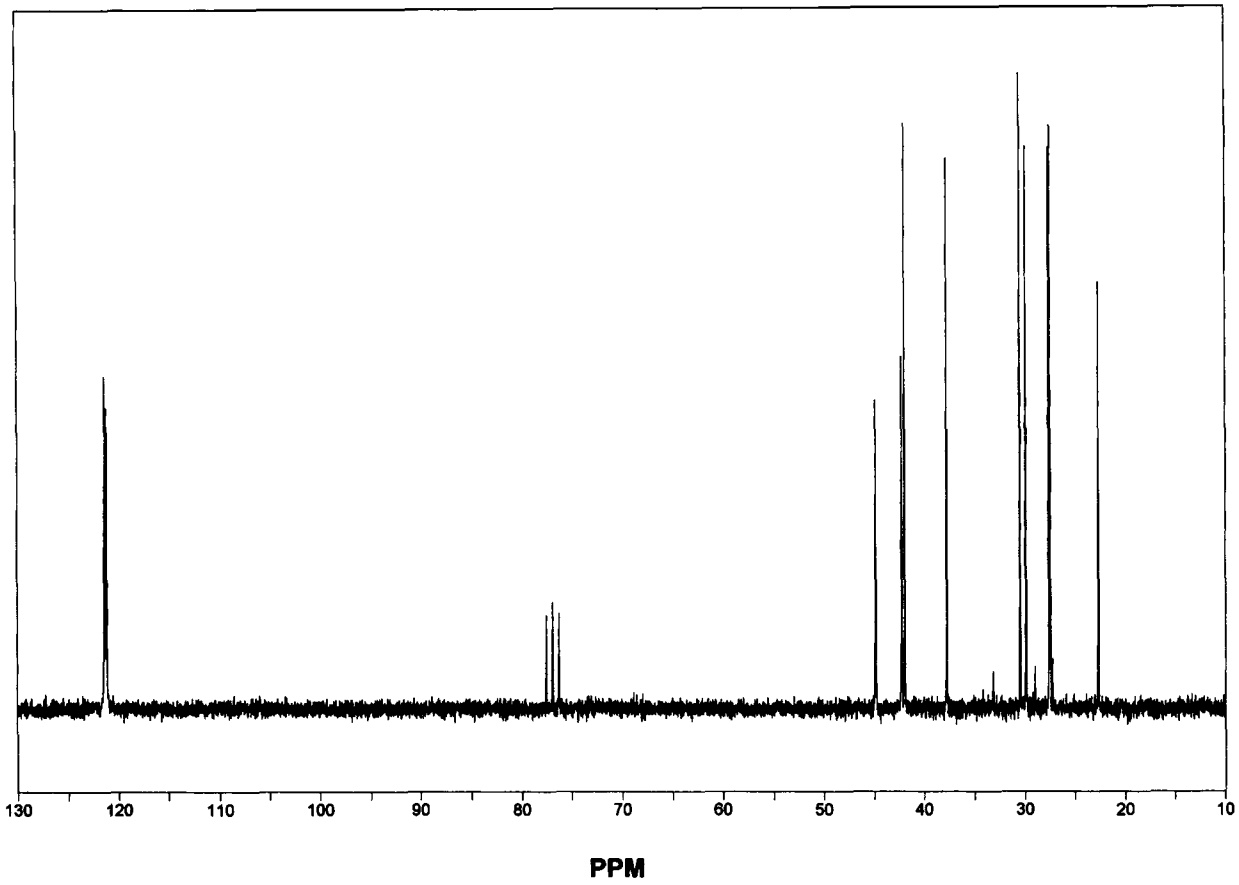

Figure 3 ^{13}C spectrum of triamininononane trisisocyanate (TTI).

spectrum of TTI, while the second section contains the ^{13}C T1 results, which were part of the foundation necessary for accurate NMR kinetic measurements. Following this, the actual kinetic work will be discussed, including a comparison of the effects of catalysis, the changes in rate with the addition of chloroform, and the effect of varying the TTI to *n*-butanol ratio. Finally, possible applications for the kinetic data will be discussed.

Assignment of ^{13}C Spectrum of TTI

The ^{13}C spectrum of TTI is shown in Figures 3 through 5, and the DEPT experiment of TTI in Figure 6. The numbering scheme for the TTI carbons is shown below:

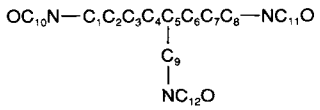

Numbering Scheme for Triamininonane Trisisocyanate (TTI)

Figure 4 shows the isocyanate region of TTI. There are two isocyanate peaks in this region. The more intense NCO peak at 121.4 ppm arises from TTI Carbons 10 and 11, while the peak at 121.2 ppm arises from TTI carbon 12. The ^{13}C and DEPT experiments for the methylene/methine region of TTI are shown in Figures 5 and 6. Based on this, the C5 methine carbon was assigned to the peak at 37.7 ppm. Assignment of many of the remaining peaks was based on chemical shift calculations using the Grant–Paul additivity rules[15] and the use of a similar compound spectrum found in the literature,[16] triaminooctane trisisocyanate (TAO–TI). TAO–TI with its numbering scheme is shown below:

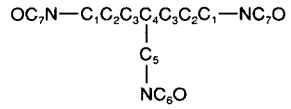

Numbering Scheme for Triaminooctane Trisisocyanate (TAO-TI)

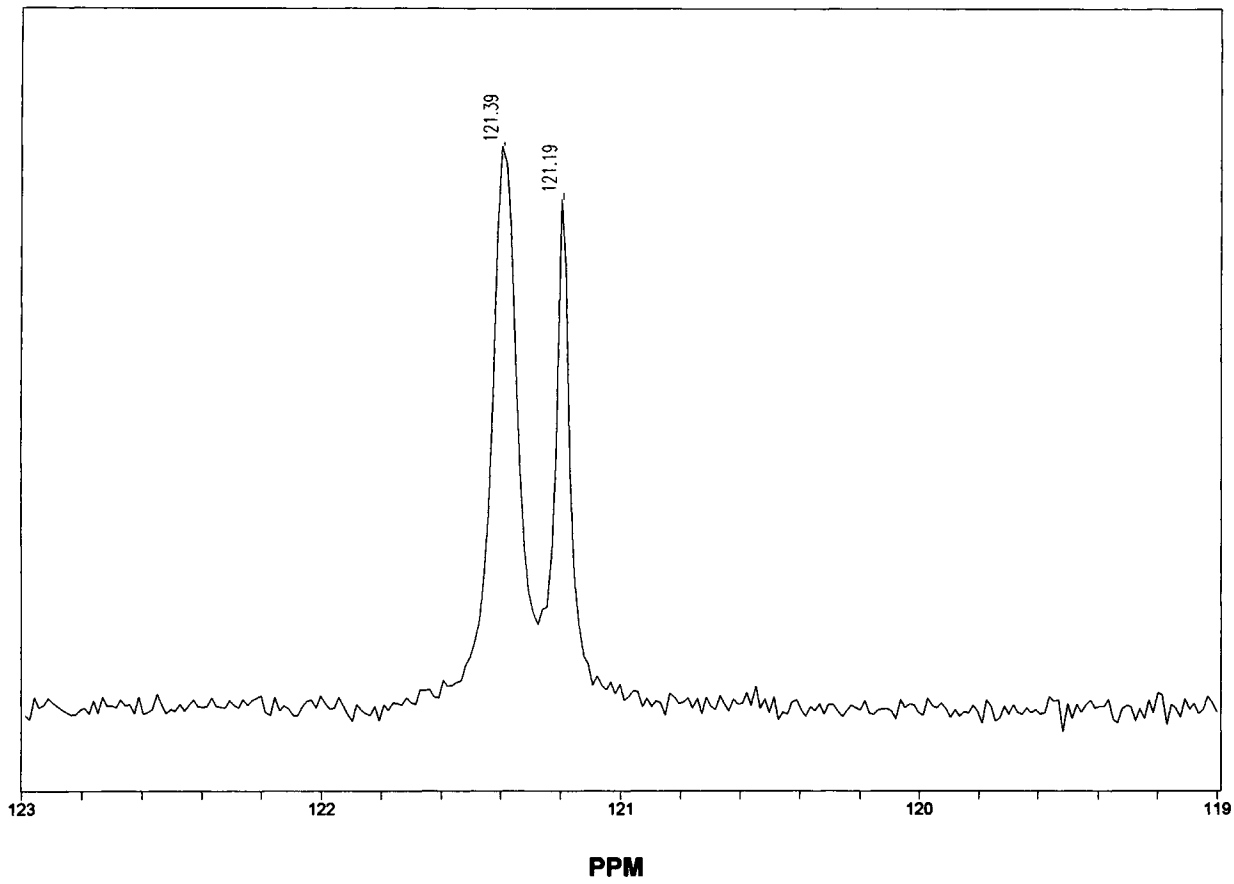

Figure 4 ^{13}C spectrum of isocyanate region of TTI.

It was necessary to account for any referencing differences between our TTI work and the literature work for TAO–TI. The equivalent TAO–TI carbon peaks are shifted downfield by 0.5 ppm for the isocyanate (121.9 ppm for TAO–TI vs. 121.4 ppm for TTI) and the methine carbons (38.2 ppm for TAO–TI vs. 37.7 ppm for TTI). Thus, we subtracted 0.5 ppm from our shifts to compare against TAO–TI chemical shifts. This was invaluable in separating subtle differences in chemical shifts of different TTI carbons. The full set of TAO–TI ^{13}C-NMR assignments is contained in Table I.

Assignment of the remaining TTI carbons is shown in Table II. The peak at 44.9 ppm in Figure 5 is to TTI carbon C9; this is based primarily on chemical shift calculations. TTI Carbons C8 and C1 are assigned to the peaks at 42.3 and 42.0 ppm, respectively. The assignment of the peak at 42.3 ppm to TTI carbon C8 is supported by the ^{13}C work on TAO–TI, which has a peak at 42.4 ppm (after correcting for referencing). The peak at 22.6 arises from TTI carbon C3, as this shift is sufficiently unique to be easily assigned. TTI Carbons C6 and C7 should have comparable peaks in the TAO–TI spectrum. TAO–TI contains peaks at 27.9 and 27.7 ppm (after correcting for referencing); thus, the TTI peaks at 27.6 and 27.5 ppm arise from carbons C6 and C7, respectively. The peaks at 30.5 ppm and 29.9 are, therefore, due to TTI carbons C2 and C4, respectively, as TTI C2 would be expected to appear further downfield than TTI carbon C4. It should be noted that the order of C6/C7 and C2/C4 are based on their relative positions in the chemical shift calculations, and it may be possible that the assignments for these two sets of peaks are reversed. These peaks were not used in this study, and as such a misassignment would not affect the conclusions of this work.

^{13}C T1 Results

Quantitative ^{13}C-NMR requires that the recycle delay be five times the longest T1 value in the system.

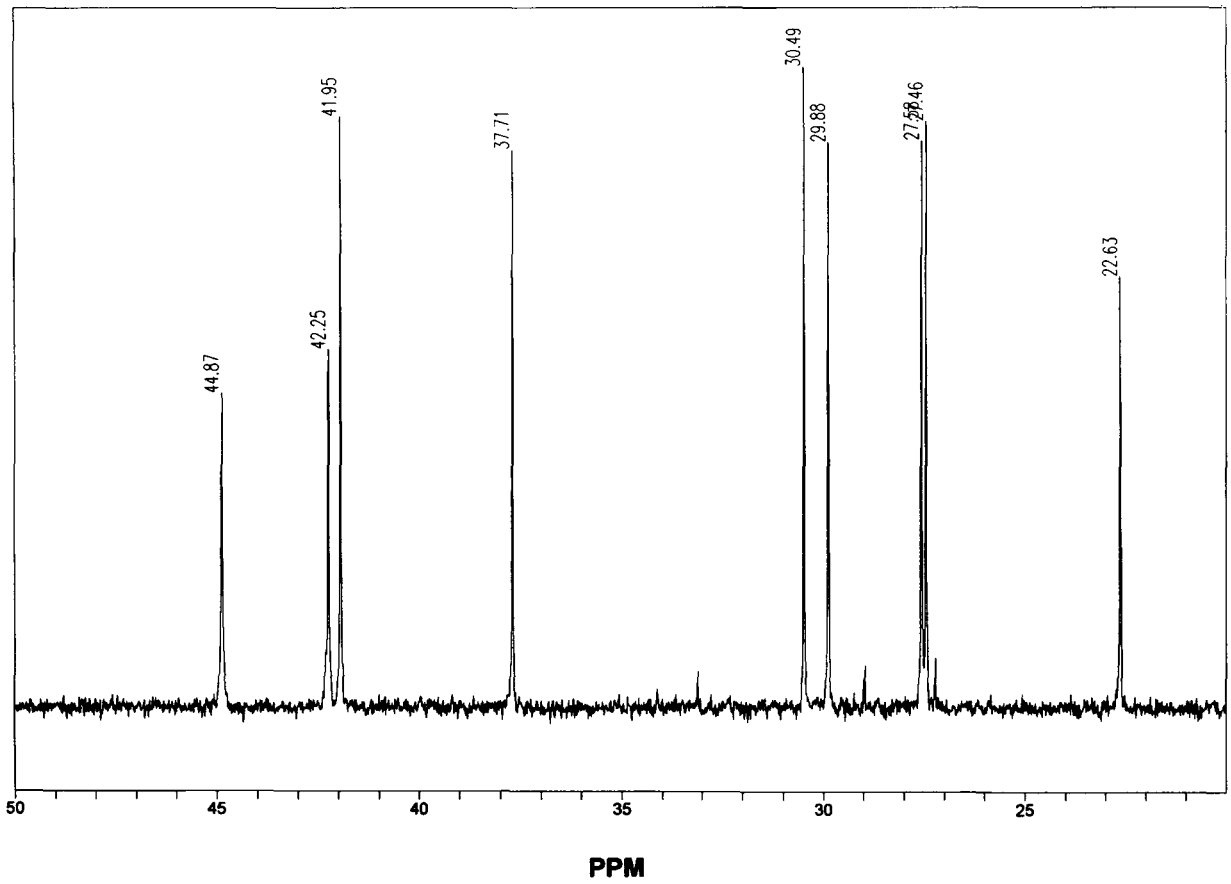

Figure 5 ^{13}C spectrum of aliphatic region of TTI spectrum.

This requirement necessitated the measurement of the ^{13}C T1 values for several different carbons: the isocyanates carbons C10/C11 and C12, and the methylene carbons C1, C8, and C9 in TTI, and the *n*-butanol carbons C1–C4. Table III lists the ^{13}C T1 values for the methylene carbons adjacent to the isocyanates, while Table IV lists the values for the *n*-butanol carbons. The isocyanates carbons have extremely long ^{13}C T1 values (approximately 10 s or longer); coupled with the lack of resolution of the C10/C11 carbons makes these peaks poor choices for kinetic measurements. The *n*-butanol carbons in Table IV are also very long when compared to the TTI methylene carbons in Table I. Based on these considerations, the decision was made to use the TTI methylene carbons C1, C8, and C9 to quantify the kinetics of the *n*-butanol/TTI reaction. Furthermore, the long ^{13}C T1 values for *n*-butanol meant that the *n*-butanol concentration could not be directly measured without significantly impacting the precision of the kinetic measurements (by increasing the recycle delay and minimizing the number of scans).

Kinetic Measurements

The kinetic measurements were performed under a variety of experimental conditions. The first key to performing kinetic measurements was to determine over which range of concentrations the rate constant should be calculated. Figure 2(a–c) contains typical plots of $-d[Ai]/dt$ vs. $[Ai]^*[BuOH]$. In this system we chose to limit the rate constant calculation to points above a $[Ai]^*[BuOH]$ value of 3.5 (which corresponds to a conversion of 75–80%). In some of the systems studied (notably the catalyzed systems) there is a second slope at higher conversions. This second slope is most likely due to the change of the polarity of the system with conversion of isocyanate and alcohol to carbamate, though the effect of viscosity cannot be ruled out. This deviation from linearity has been observed by several other authors,[5,7,9,13] although their explanations do not necessarily agree with ours. The general explanation is that the presence of urethane groups on the same molecule or in sufficient quantity in solution interacts with the reactants and changes the rate con-

stants. If the effect was due to reaction of other NCO groups on the same TTI molecule, this deviation from linearity would be observed at much lower conversions.

The results for the uncatalyzed and catalyzed rate constants are shown in Table V. The differences in reactivity between the three isocyanates groups in the uncatalyzed system are small, but a large difference can be seen for the catalyzed system for the C9 carbon, which is the short branch system. This is probably due to steric considerations involving the interaction between the isocyanate and the DBTDL catalyst. Whether the isocyanate or the alcohol are forming a complex with the DBTDL catalyst is not exactly clear for our data or the literature data. In either case, the complex could be easily hindered from reaction due to the branch site near the C9 carbon.

Figures 7 and 8 are a graphic illustration of the negative log of the kinetic constants as function of 1/T. This is an activation energy plot used for calculating activation energies for these reactions. All of the peaks in the uncatalyzed system exhibit some deviations from simple Arrhenius behavior, while the catalyzed system shows much better correlation with

Table I ^{13}C-NMR Assignments for Triaminooctane Trisisocyanate (TAO-TI)

Carbon	Peak Position (ppm)
1	42.9
2	28.4
3	28.2
4	38.2
5	45.7
6	121.9
7	121.9

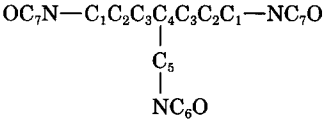

Numbering Scheme for Triaminooctane Trisisocyanate (TAO-TI).

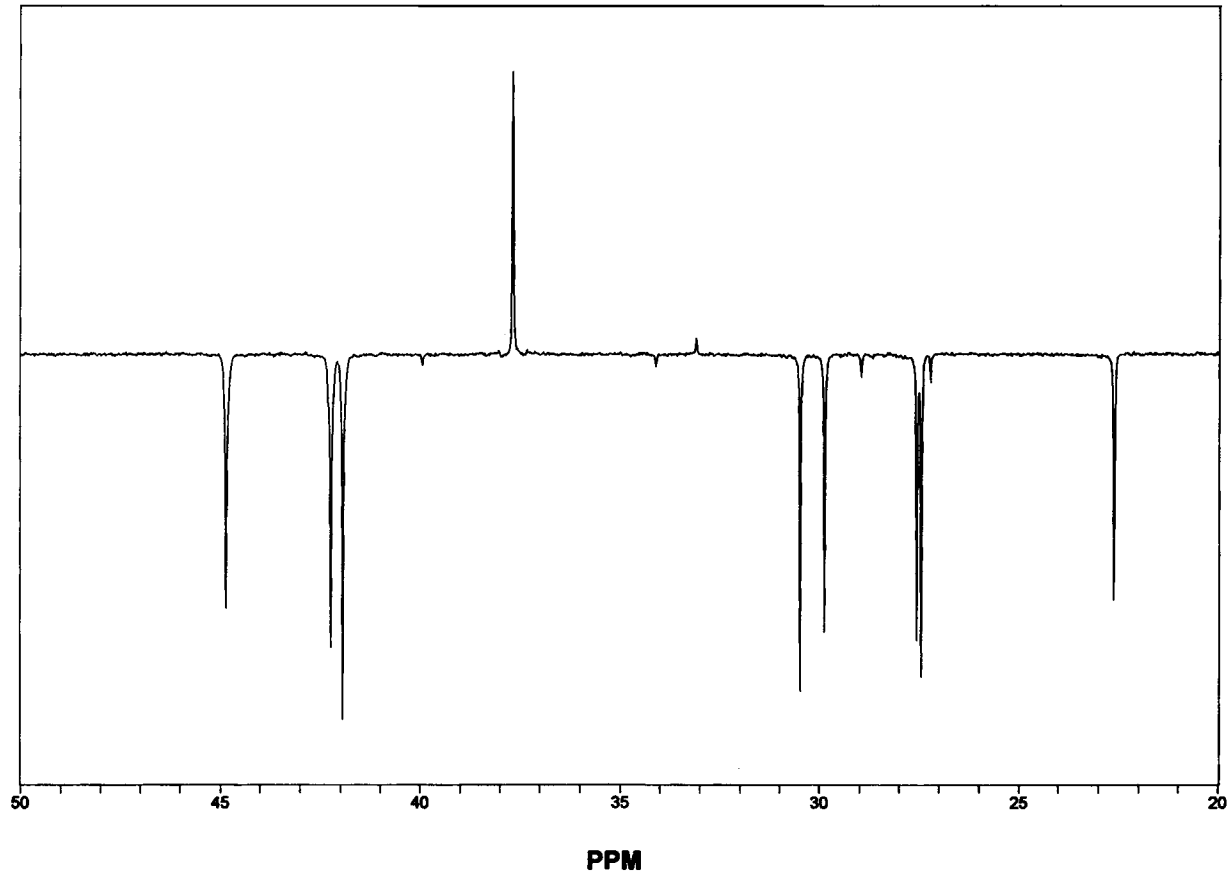

Figure 6 DEPT spectrum of aliphatic region of TTI.

Table II ^{13}C-NMR Assignments and Calculations for Triaminononane Trisisocyanate (TTI)

Carbon	Calculated Chemical Shift (ppm)	Measured Chemical Shift (ppm)
1	44.0	42.0
2	31.9	29.9/30.5
3	25.3	23.3
4	32.1	30.5/29.9
5	43.7	37.7
6	30.0	27.6/27.5
7	29.0	27.5/27.6
8	44.2	42.3
9	48.6	44.9
10	N/A	121.4
11	N/A	121.4
12	N/A	121.2

$OC_{10}N—C_1C_2C_3C_4C_5C_6C_7C_8—NC_{11}O$
C_9
$NC_{12}O$

Numbering Scheme for Triaminononane Trisisocyanate (TTI).

Arrhenius behavior. Table VI shows the activation energies calculated assuming pure Arrhenius-type behavior. It is interesting to note that the activation energies for the uncatalyzed system decrease with increasing chain length. This is probably due to increased motional freedom allowing for a more rapid reaction rate. This is supported by the ^{13}C T1 results in Table III; the increase in T1 values from the short branch (C9) to the long branch (C1) are due to an increase in molecular motions, as TTI would be expected to be on the fast side (small τ_C, near point D) of the T1 curve shown below.[17,*] This curve is the relationship between the average correlation time τ_C and the measured T1 value; an increase in T1 corresponds to an increase in localized molecular motions (if the system is on the fast side of the curve):

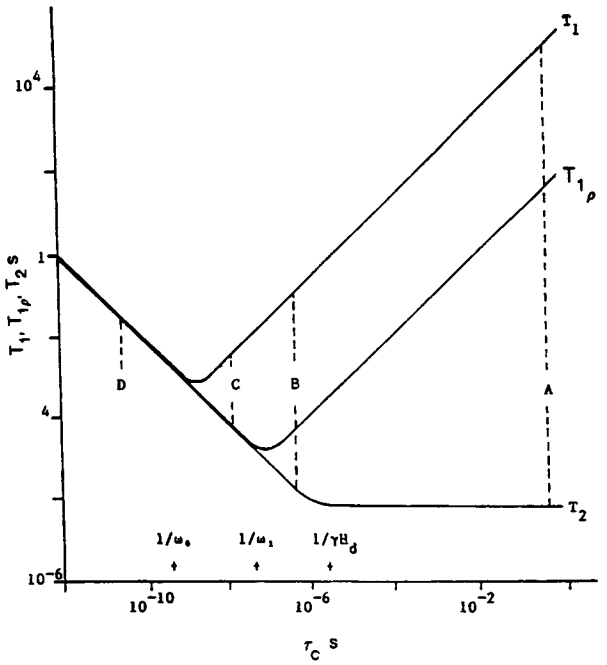

The drop in activation energy with increasing chain length in the uncatalyzed system is in contrast to the catalyzed system, where the short branch has the lowest activation energy. We believe this is an effect of the catalyst interaction (easier to bind a short chain then longer chain). Our hypothesis is that in the catalyzed systems the activation energy represents the energy of disassociation of the catalyst–reaction complex, while the overall rate constant is more representative of the rate of formation of the complex. This helps to explain why the short branch system (Carbon C9) has a low activation energy yet also has the smallest rate constants.

Table VII shows the effect of varying the butanol : TTI ratio. Increasing the butanol : TTI ratio increases

Table III ^{13}C T1 Values for TTI as a Function of Temperature

Peak	25°C	35°C	45°C	55°C
Carbon 9 [44.8 ppm]	451	655	602	680
Carbon 8 [42.1 ppm]	855	1202	1170	1412
Carbon 1 [41.8 ppm]	959	1307	1329	1564

T1 values in milliseconds.

Table IV ^{13}C T1 Values for *n*-Butanol as a Function of Temperature

Peak	25°C	35°C	45°C
C1	3.51	4.58	5.08
C2	4.45	5.33	6.10
C3	6.30	7.79	8.12
C4	6.47	7.09	7.80

T1 values in seconds.
Numbering scheme for *n*-butanol carbons:

$C_1—C_2—C_3—C_4—OH$

Table V Rate Constants for TTI/*n*-Butanol System Catalyzed and Uncatalyzed TTI : BUOH Ratio of 1.5 : 1, Chloroform as Compatibilizing Agent

	k (Short)	*k* (Medium)	*k* (Long)	*k* (Total)
Uncatalyzed				
25°C	9.9E-06	1.3E-05	1.3E-05	3.6E-05
35°C	1.4E-05	2.0E-05	1.8E-05	5.3E-05
45°C	4.0E-05	4.3E-05	2.9E-05	1.1E-04
Catalyzed				
25°C	2.6E-05	5.3E-05	4.7E-05	1.3E-04
35°C	4.8E-05	1.1E-04	1.2E-04	2.8E-04
45°C	6.9E-05	2.5E-04	2.5E-04	5.7E-04

Units = liter/(mol × seconds).

the overall rate constants; this is due to the increased polarity of the solution in the presence of increased amounts of *n*-butanol. The isocyanate–alcohol reaction is a nucleophilic attack; increasing the solution polarity will tend to favor nucleophilic reactions.

Table VIII illustrates the effect of chloroform on the rate constants. In the absence of chloroform, the rate constants are significantly depressed. Chloroform is necessary in these systems to maintain a single-phase system; in the absence of any chloroform the system will exhibit two phases until a small amount of reaction has occurred, at which point the system forms 1 phase. Thus, the depressed rate constants in the absence of chloroform are probably due to the fact that the reaction is more interfacial then homogeneous initially in the absence of chloroform.

A comparison between our kinetic constants and those in the literature was difficult at best. Isocyanate–

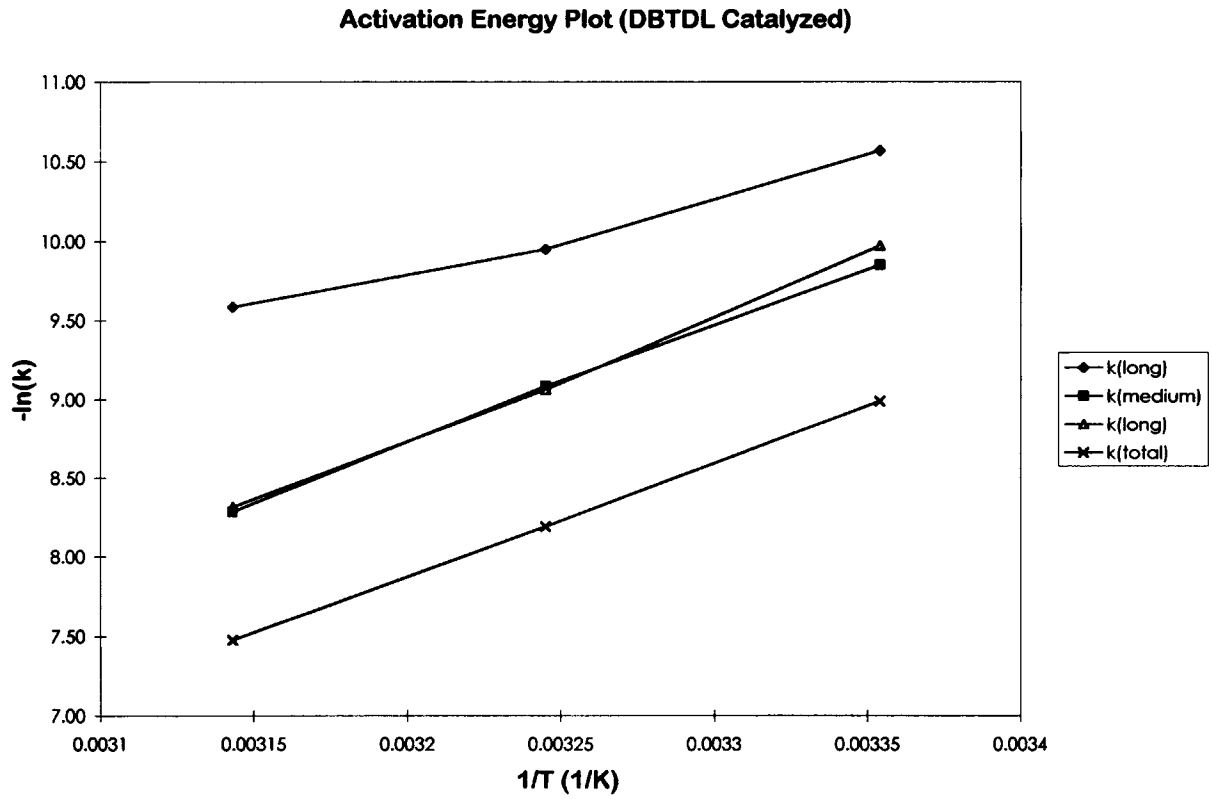

Figure 7 Rate constants as function of 1/T for the uncatalyzed system.

alcohol reactions are highly sensitive to variations in reaction conditions including (but not limited to) type of solvent, reactant concentration, and ratio of reactants. The literature values, which were done in dilute solutions in most cases, were substantially lower then the values we obtained. Thus, meaningful direct comparisons of our work to the literature is difficult.

A possible application of this work is the production of linear (relatively) carbamates with branch isocyanate functionality. The rate difference between the medium/long branches and the short branch in the catalyzed system at 45°C is a factor of 3.5. This is great enough to allow the selective conversion of the medium and long branches while highly limiting the amount of reaction of the short branch. This could be used to produce a linear carbamate with branch functionality to allow crosslinking in the coating formulation. There may even be catalyst systems with a greater separation in rates for TTI; a systematic study of catalysts for TTI would be very useful in this regard.

CONCLUSIONS

Under DBTDL-catalyzed conditions there is a difference in second-order rate constants between the short-branch isocyanate group vs. the medium and long branch isocyanate groups. This difference is not observed in the uncatalyzed system. Changing the polarity of the system by adding or excluding chloroform and changing the butanol : TTI ratio also affects the rate constants; chloroform and additional butanol both increase the rate constants. This is due to the high sensitivity of isocyanate reactions to solution polarity. The activation energy increases with increasing chain length in the uncatalyzed system, while the long and medium branches have similar (and higher) activation energies than the short branch in the DBTDL-catalyzed system. This difference is probably due to the effect of catalyst–reac-

Table VI Calculated Activation Energy

	Ea (kJ/mol)
Short Branch Uncatalyzed	55
Medium Branch Uncatalyzed	46
Long Branch Uncatalyzed	31
Total Uncatalyzed	44
Short Branch Catalyzed	39
Medium Branch Catalyzed	62
Long Branch Catalyzed	65
Total Catalyzed	60

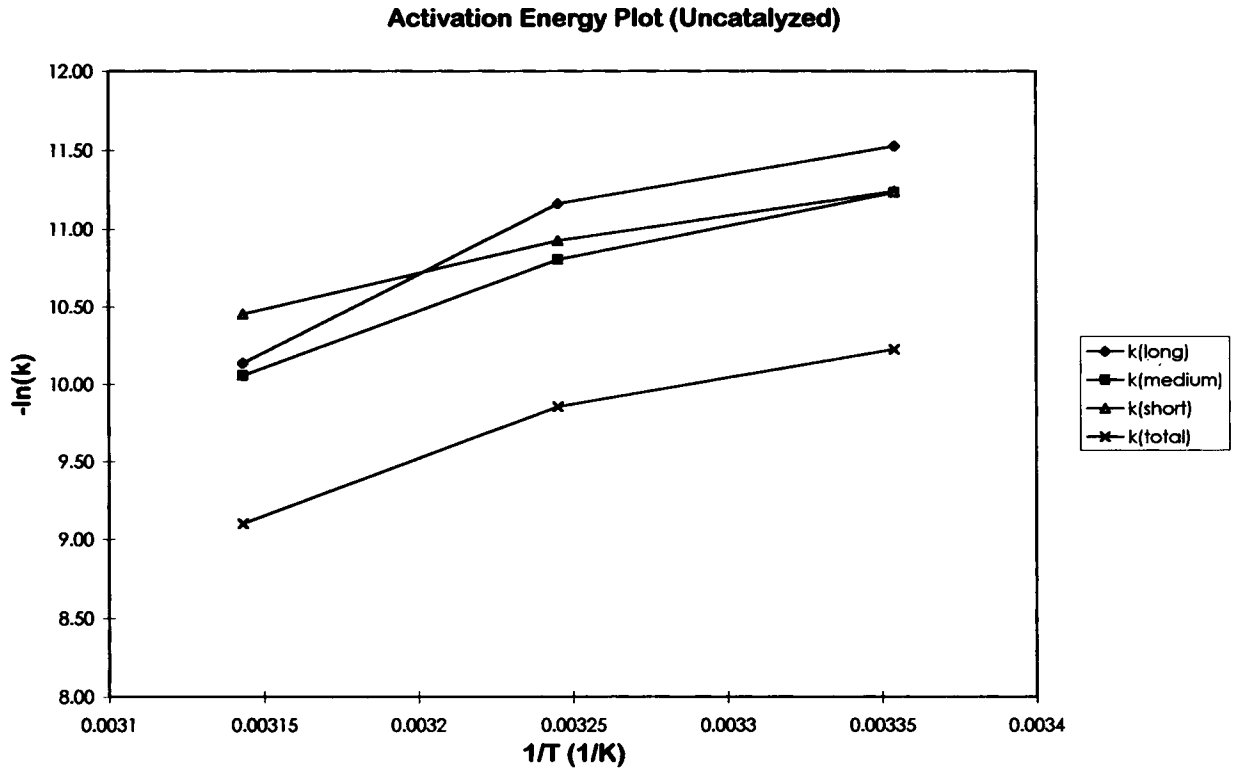

Figure 8 Rate constants as function of 1/T for the DBTDL system.

Table VII Effect of BuOH : TTI Ratio on Rate Constants

	k (44.8)	*k* (42.1)	*k* (41.8)	*k* (Total)
35°C with CDCL3	1.4E-05	2.0E-05	1.8E-05	5.3E-05
35°C without CDCL3	6.7E-06	7.0E-06	5.8E-06	2.0E-05
45°C with CDCL3	9.4E-05	5.0E-05	4.2E-05	1.9E-04
45°C without CDCL3	1.0E-05	1.1E-05	8.8E-06	3.0E-05

Units = liter/(mol × seconds).

Table VIII Effect of *n*-Butanol : TTI Ratio on Rate Constants

	k (44.8)	*k* (42.1)	*k* (41.8)	*k* (Total)
25°C, BuOH : TTI 1 : 1	6.7E-06	8.7E-06	6.5E-06	2.2E-05
25°C, BuOH : TTI 1.5 : 1	9.9E-06	1.3E-05	1.3E-05	3.6E-05

Units = liter/(mol × seconds).

tant disassociation in the catalyzed samples and chain end mobility differences in the uncatalyzed systems.

The authors would like to thank Robert T. Jones of the Specialty Resins group of the Industrial Products Group for his support of this work, William McGhee of Monsanto Corporate Research for supplying the TTI used in this study, Roger Ayotte, Lora Spangler (Physical and Analytical Sciences Center, Chemical Group of Monsanto), and Loren Hill (Speciality Resins group) for there useful discussions and suggestions in regards to the kinetics calculations and results.

REFERENCES

1. R. T. Wojcik, *Mod. Paint. Coat.*, **83**(7), 39 (1993).
2. T. E. Waldman and W. D. McGhee, *J. Chem. Soc., Chem. Commun.*, **29,** 957 (1994); W. D. McGhee, T. E. Waldman, U.S. Pat. 5,189,205.
3. M. Ojunga-Andrew, H. P. Higginbottom, and L. W. Hill, *Proc. of Twenty Fifth Waterborne, Higher Solids and Powder Coatings Symposium,* Feb. 22–24, 1994, New Orleans, LA.
4. I. Yilgor and J. E. McGrath, *J. Appl. Polym. Sci.*, **30,** 1733 (1985).
5. G. Anzuino, A. Piro, G. Rossi, and L. Polo Friz, *J. Polym. Sci., Polym. Chem. Ed.*, **13,** 1667 (1975).
6. K. C. Frisch, S. L. Reegan, and B. Thir, *J. Polym. Sci., Part C,* **16,** 2191 (1967).
7. S. D. Seneker and T. A. Potter, *J. Coat. Technol.*, **63**(793), 19 (Feb. 1991); *Proc. of Twentieth Waterborne and Higher-Solids Coatings Symposium,* Feb. 1–3, 1989, New Orleans, LA, pp. 369–376.
8. E. P. Squiller and J. Rosthauser, *Mod. Paint. Coat.*, **77**(6), 28 (1987); *Polym. Mater. Sci. Eng.*, **55,** 640 (1986); *Proc. of Eighteenth Waterborne and Higher-Solids Coatings Symposium,* Feb. 25–27, 1987, New Orleans, LA, pp. 460–476.
9. A. E. Oberth and R. S. Bruenner, *Ind. Eng. Chem. Fund.*, **8**(3), 383 (1969).
10. J.-J. Tondeur, G. Vandendunghen, and M. Watelet, *J. Chem. Res. (S)*, 262 (1992).
11. A. G. Kozhevov, Ye. V. Genkina, and Ya. A. Shmidt, *Vysokomol. Soedin.*, **A14**(3), 662 (1972).
12. F. W. Abbate and H. Ulrich, *J. Appl. Polym. Sci.*, **13,** 1929 (1969).
13. F. Surivet, T. M. Lam, and J.-P. Pascault, *J. Polym. Sci., Part A: Polym. Chem.*, **29,** 1977 (1991).
14. C. J. Pouchert and J. Behnke, *The Aldrich Library of ^{13}C and ^{1}H FT NMR Spectra,* Aldrich Chemical Company, Milwaukee, WI, 1993.
15. R. M. Silverstein, G. C. Bassler, T. C. Morrill, *Spectrometric Identification of Organic Compounds*, 4th ed., Wiley, New York, 1981.
16. J. W. Gilman, Y. A. Otonari, and R. D. Chapman, *Polym. Bull.*, **27,** 59 (1992).
17. J. L. Koenig, *Spectroscopy of Polymers,* American Chemical Society, Washington, DC, 1992, p. 260.

Received January 31, 1995
Accepted April 11, 1995